Torque Ripple Reduction in Five-Phase Induction Machines Using Mixed Winding Configurations

M. Muteba, A.A. Jimoh and D. Nicolae

***Abstract* - In this paper, the authors take a particular look at the effects of combination of different stator winding configurations in a 40 stator slots, 2-pole, and five-phase induction machine. They show, through computer simulation, that the combination of double and triple layer with 19/20 coil pitch reduced the torque ripple from 19.1%, for the conventional single layer full pitch, and from 10.6 %, for the conventional double layer with 19/20 coil pitch having the same rating, down to 8.7 % while maintaining the torque average. The same has to be said for the double combination which is the combination of double and triple layer combined with slot shift and coil side shift in one slot having 9/10 coil pitch. This double combination reduces tremendously the torque ripple from 28.8 %, for a conventional double layer 9/10 coil pitch, down to 10.2 % and still maintained the torque average. Some other winding combinations reduce both average and torque ripple.**

***Keywords*—**Five-phase induction machines, Phase-belt, Torque ripple, Winding combinations.

I. Introduction

THE airgap field distribution in induction machines (IMs) is influenced by the stator and rotor magneto-motive force (MMF) distribution and magnetic saturation in stator and rotor teeth and back cores. The placement of windings in slots leads to a stepped-like waveform of the stator or rotor MMFs which exhibit space harmonics [3].

Most electric machine designs rely on the fundamental flux wave theory. Attention is concentrated on the achievement of sinusoidal flux density in the airgap with as little harmonic content as possible. The fundamental component of resultant airgap flux density distribution in interaction with the fundamental of stator or rotor MMF produces the fundamental electromagnetic torque in IMs.

However, very early IMs had two phases, but the three-phase version very soon replaced these, and this eliminated the third harmonic problems associated with two-phases and resulted in a motor that was generally better in all performance aspects [5]. Increasing the number of phases beyond three, though may be costly, has advantages which might be worth considering for certain special applications [4]. Among the advantages of machines with more than three-phases are to improve the shape of the fundamental flux wave by eliminating significantly some space harmonics, to reduce torque ripples and rotor harmonic power loss for inverter supply motors and to improve reliability since loss of one of many phases does not prevent the motor from starting and running [2].

The torque ripple results from the fact that discreet spatial distribution of windings does not produce an exactly sinusoidal magneto motive force (MMF). The actual MMF wave contains significant number of higher order space harmonics. Their presence results in torque ripple that varies as a function of the number of slots, these space harmonics are commonly called slot harmonics. Another source of torque ripple is localized saturation of the magnetic material [8]. Previous research has shown that the torque ripple could be eliminated to a certain extent by short pitching the winding, by typically one or two slots to reduce lower-order MMF space harmonics [6]. Although this method has proved itself worthy but was limited to coil chording of conventional double-layer windings and slot skewing.

In this paper the authors look at possible combination of different winding configurations and their effect on the torque ripple. Though the study is limited to a particular five-phase machine, the approach is valid for any m-phase induction machine of p-number of poles with integer number of slots per pole and per phase. The different winding configurations and different combinations investigated in this paper are found in Appendix table V.

However, the winding configurations do not affect the slot harmonics but have impact on phase-belt harmonics which depend on the placement of conductors under different phase-belts. Before proceeding further, the following assumptions are taken into consideration.

- Only the space phase-belt primary sequence harmonics are investigated.
- The machine is considered to be operating in steady state under no-load condition.
- Saturation effects are neglected, thus the space harmonics produced by leakage saturation and saturation of main flux are not considered.
- Effects of slot stator and rotor slot openings are neglected.
- The five-phase stators current are assumed to be sinusoidal.
- There is no skew.

II. Phase-Belt Harmonics

For five-phase symmetrical windings with integer q slots per pole and phase, even order harmonics are zero and multiples of five are also zero. The existence of *"n"* primary sequence and secondary sequence order space harmonics and their direction of rotation in the air-gap of the five-phase induction machine are found as in (1) and (2), respectively [1].

M. Muteba is with Tshwane University of Technology, Department of Electrical Engineering, Private bag X680, 0001, Pretoria, South Africa (e-mail: mbikachris@webmail.co.za).
A. A. Jimoh is with Tshwane University of Technology, Department of Electrical Engineering, Private bag X680, 0001, Pretoria, South Africa (e-mail: jimohaa@tut.ac.za).
D. Nicolae is with Tshwane University of Technology, Department of Electrical Engineering, Private bag X680, 0001, Pretoria, South Africa (e-mail: danaurel@yebo.co.za).

978-1-4673-0142-8/12/$26.00 ©2012 IEEE

$$n = 10k_j + 1 \quad (1)$$

$$n = 5k_i + 2 \quad (2)$$

Where k_j is any positive or negative integer and K_i is any positive and negative odd number but not zero. The primary sequence space harmonic orders are "1, -9, 11, -19, 21, -29, 31 ..." and secondary sequence space harmonics orders are "-3, 7, -13, 17, -23, 27…". The negative sign indicates the backward direction of rotation respect to the fundamental MMF.

The space harmonics of the MMF that are investigated in this paper are due to both placement of conductors in slots and placement of various phases as phase belts under each pole. In five-phase the phase belt spread is π/5 electrical radian (one fifth of a pole). Although the effect of stator and rotor slotting influence also on the MMF stepwise distribution [6]. The effect depends on the number of slots of each member as indicated in (3) and (4).

Let us note that the slot harmonics are not investigated in this paper but are only cited to give clear explanation about the phase-belt harmonics.

$$n_s = k(Q_S / p_1) + 1 \quad (3)$$

$$n_r = k(Q_r / p_1) + 1 \quad (4)$$

Where n_s and n_r are stator and rotor slots harmonics, respectively. p_1 is the stator fundamental pole pair, Q_s and Q_r are the number of stator slots and rotor bars , respectively. It is important to note that the MMF harmonics, whose order is lower than the first stator slot harmonics as in (3), are called phase belt harmonics. For a 2-pole, 40 stator slots, five-phase induction machine the first stator slot harmonic order is 39.

The phase belt or phase band may be defined as the group of adjacent slots belonging to one phase under one pole pair. The angle subtended by one phase group is called phase spread and it is computed as in (5). The stator coil pitch is normally chosen so as to reduce the lowest order phase belt harmonics which are generally largest [6]. It is important to note that the phase belt harmonics which can exist in the partial distribution of flux are those for which the harmonic order number "n" satisfies as in (6).

$$\sigma = q \times \alpha_s \quad (5)$$

$$n_p = 2(\pi / \sigma)k_i + 1 \quad (6)$$

Where q is the average number of slot per pole and phase σ is the phase-belt angle (electrical radian) and α_s is the slot pitch angle (electrical radian). The first six space phase belt harmonics order are therefore "- 9, 11, -19, 21, -29 and 31". It is noticeable that these are primary sequence space harmonic.

Though saturation effects are neglected in this paper but one must note that in five-phase induction machine the most significant induction harmonic component that effectively produce the torque is the third one[12]. This harmonic field can be generated by saturation effect or current injection and it is part of set of secondary sequence space harmonics. These secondary sequence space harmonics are produced when winding is fed from an alternative sequence, feeding the winding with primary sequence will inherently cancel these harmonics [1].

II. WINDING ANALYSIS

A. *Basic single and double layer five phase windings*

Conventional windings for poly-phase induction machines are layed out in one or two-layers in stator slots. The total number of coils equals half the number of stator slots for single layer configurations and equal to number of stator slots in double-layer configurations. Full-pitched and short-pitched are used depending on the application. Windings are built with integer or fractional slots per pole and per phase. In this paper only integer slots per pole and phase are investigated. Fig. 1 shows a double-layer with 9/10 coil pitch of a five-phase, 40 slots, two-pole induction machine and the distribution and pitch factor are calculated as in (7) and (8), respectively [7]. The winding factor is found by doing the product of (7) and (8).

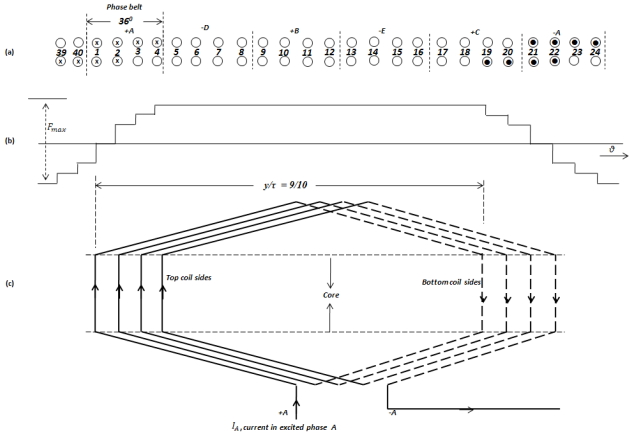

Fig.1 Double-layer (DL-9/10) Five-phase windings accommodated in 40 slots, only 26 slots are shown; (a) Double-layer slot/phase allocation , (b) winding functions, (c) coils of phase A, only 4 coils are shown.

$$K_{dn1} = \frac{\sin nq(\alpha_s / 2)}{q \sin n(\alpha_s / 2)} \quad (7)$$

$$K_{pn} = \sin n(\pi y / 2\tau) \quad (8)$$

Where K_{dn1} is the harmonic "n" distribution factor of conventional single or double layer winding, K_{pn} is the harmonic "n" pitch factor of conventional chorded double layer winding and the ratio y/τ is the coil span. Single-layer windings are build with unity coil pitch, thus the winding factor equals to the distribution factor.

B Proposed double layer windings with combination of slot shift and coil side shift in a slot

In this section, the authors present the combination of slot shift and coil side shift in the same winding. The method consists of shifting in one pole pitch the lower layer of the coil with a coil side transfer to the upper layer and in the other pole pitch the upper layer of the coil is shifted with a coil side transfer to the lower layer as shown in Fig.2.

It is clearly indicated that the distribution factor is calculated using the average number of slots per pole and per phase as in (9). "Equation (8) is valid for slot pitch shift but not valid for coil side shift in a slot".

$$q = (q_1 + q_2)/2 \tag{9}$$

Where q_1 and q_2 are the number of slots per pole and per phase of different layers of coil side shift

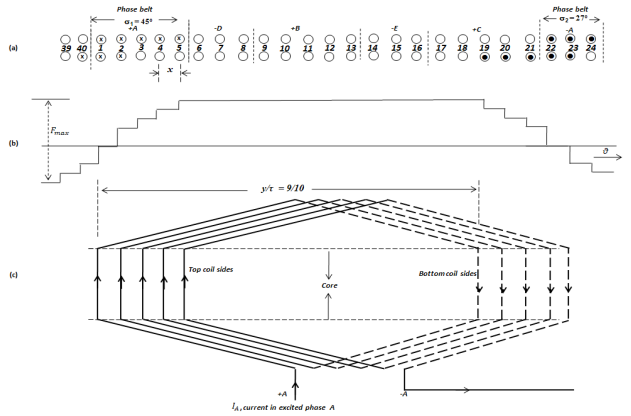

Fig.2. Double-layer (DLSC-9/10) Five-phase windings accommodated in 40 slots, only 26 slots are shown; (a) Double-layer with coil side shift in an upper slot, slot/phase allocation , (b) winding functions, (c) coils of phase A, only 5 coils are shown

From Fig.2, it is clear that by applying slot pitch shift and coil side shift in a slot that the equivalent reduction 'x' of a coil span for a winding with coil side shift can be written as in (10).

$$x = \tau - (y/\tau) = [(q_1 - q_2)/2] \times \alpha_s \tag{10}$$

$$(\pi y)/\tau = 1 - (p_1/Q_s)(q_1 - q_2) \tag{11}$$

The winding corresponds to the slot pitch shift in the ratio $\pi y/\tau$. By substituting (11) in (8) we obtain the harmonic "n" pitch factor of the coil side shift in a slot as:

$$K_{cn} = \sin\left\{ n\left[1 - (p_1/Q_s)(q_1 - q_2)\right]\frac{\pi}{2}\right\} \tag{12}$$

The harmonic "n" winding factor of the combination of slot pitch shift and coil side shift in a slot is the product of (7), (8) and (12). Other important member in (12) is $(q_1\text{-}q_2)$ that will depend on the number coil sides shift in other slots.

C Proposed Combination of double and triple layer

By employing the combination of double and triple layer, some slots have conductors belonging to two different phases. One phase is made of half coil and the other phase is made of one and half coil. The currents in these phases are out of phase with each other by either $4\pi/5$ electrical radian or $6\pi/5$ electrical radian.

Therefore the net currents and leakage flux are less than for slots with current belonging to the same phase. In a double-triple layer with 19/20 coil pitch two slots per pole and phase have current belonging to the same phase and three slots have current of two different phases which are out of phase. In a double-triple layer with 9/10, fig.3, only one slot per pole and phase has current of the same phase. All remaining four slots have current of two different phases. In a double-triple layer with 17/20 coil pitch none of the five slots have current belonging to the same phase.

The phase band in these double-triple layer windings consist now of five slots not four slots like in conventional single and double layer windings thus the new phase-belt spread is $\pi/4$ electrical radian.

As noted in section II, each slot is separated by its neighbor by slot angle "α_s" specified for the fundamental field, the effective phase separation for n^{th} harmonic is "$n\ \alpha_s$". The coils accommodated in the five slots that make the phase-belt have different field component magnitudes. Two slots house half-coil each and the other three slots house a full coil each. The harmonic "n" distribution factor of the combination of double and triple layer is than calculated as in (13) and its winding factor is the product of (13) and (8).

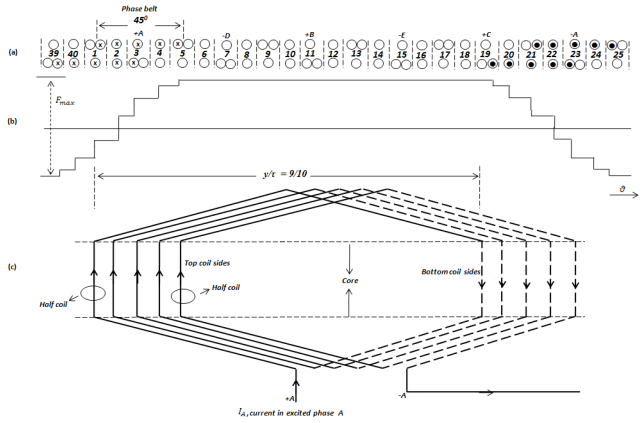

Fig.3. Double-triple-layer (DTL-9/10) Five-phase windings accommodated in 40 slots, only 27 slots are shown; (a) Double-triple layer, slot/phase allocation , (b) winding functions, (c) coils of phase A, only 4 coils are shown.

$$K_{dn2} = \frac{\sin n(q_i + q_j)(\alpha_s/2)}{(q_i + q_j)\sin n(\alpha_s/2)} \tag{13}$$

Where q_j is the number of slots per pole and phase that house half coil sides and q_i is the number of slots per pole and phase that house full coil sides only.

D. Proposed combination of double-triple layer with combination of slot shift and coil side shift in a slot

The double combination is achieved by mixing the combination of double and triple layer with the combination of slot shift and coil side shift in a slot. It is noted that in this mixed winding configuration one coil group consists of four and a half coils and the other coil group has three and half coils to make an average of eight coils per phase. The winding combination in (b) of section II of this paper has a coil group per phase of five coils and the other coil group has only three coils per phase that makes also an average of eight coils per phase.

It is noticed that the coil group distribution is not uniform for winding combinations discussed in (b) and (d) of this section but the same cannot be said for the combination of double and triple layer discussed in (c) of the same section.

The double-triple layer winding has uniform coil group distribution. Both coil groups per phase consists of three full coils and two half coils. The winding arrangement of the double-triple layer with 9/10 chorded coils combined with a coil side shift in upper slot is shown in fig.4.

The distribution factor for a combination of a double and triple layer is calculated as in (13) and the pitch factor of the coil side shift in a slot is the same as in (12). The harmonic "*n*" winding factor of double-triple layer with a combination of slot shift and coil side shift in a slot can be calculated by using (14) and the readily calculated harmonic winding factors of different winding configurations are found in table I.

$$K_{wn} = K_{dn2} K_{pn} K_{cn} \tag{14}$$

The proposed double-triple layer 19/20 coil pitch with combination with slot shift and coil side shift in a slot drops considerable the 19th and the 21st harmonic winding factors and still maintains it fundamental winding factor closer to the fundamental winding of the conventional 19/20 coil pitch double layer winding.

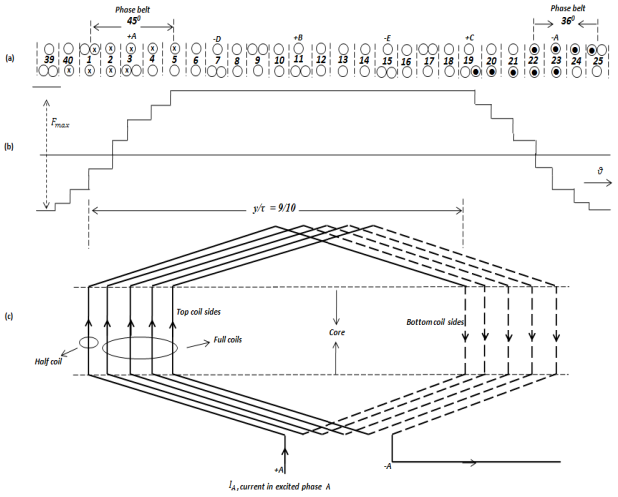

Fig.4. Double-triple-layer (DTLSC-9/10) Five-phase windings accommodated in 40 slots, only 27 slots are shown; (a) Double-triple layer with coil side shift in upper slot, slot/phase allocation , (b) winding functions, (c) coils of phase A, only 4.5 coils are shown

TABLE I
HARMONIC WINDING FACTORS

Winding Layout	n=1	n=3	n=7	n=9	n=11	n=13	n=17	n=19	n=21	n=23	n=27	n=29	n=31
	K_{w1}	K_{w3}	K_{w7}	K_{w9}	K_{w11}	K_{w13}	K_{w17}	K_{w19}	K_{w21}	K_{w23}	K_{w27}	K_{w29}	K_{w31}
SL-20/20	0.9850	0.8663	0.3871	0.1190	-0.1010	-0.2372	-0.2080	-0.0770	0.0770	0.2080	0.2372	0.1010	-0.1190
DL-19/20	0.9820	0.8423	0.3300	0.0900	0.0650	-0.1239	-0.0485	0.0060	-0.0060	-0.0485	-0.1239	0.0060	-0.0900
DL-9/10	0.9730	0.7718	0.1757	0.0180	-0.0160	0.1077	0.1853	-0.0760	-0.0760	-0.1853	-0.1077	-0.0160	0.0180
DL-17/20	0.9580	0.6587	-0.0303	-0.0620	-0.0860	0.2364	0.1351	-0.0180	0.0180	0.1351	0.2364	0.0860	0.0620
DLSC-19/20	0.9780	-0.8190	-0.2813	0.0690	-0.0420	-0.0647	-0.0113	-0.0005	0.0005	-0.0113	-0.0634	0.0420	-0069 0
DLSC-9/10	0.9690	-0.7504	-0.1498	0.0140	0.0100	0.0562	0.0432	0.0059	0.0059	-0.0432	-0.0562	0.0100	0.0140
DLSC-17/20	0.9550	0.6405	-0.0258	-0.0470	0.0560	0.1235	0.0315	0.0014	-0.0014	0.0315	0.1235	-0.0560	0.0470
DTL-19/20	0.9720	0.7695	0.1249	-0.0890	0.1580	-0.1132	0.0183	-0.0140	-0.0140	-0.0183	0.1132	0.1580	-0.0890
DTL-9/10	0.9630	0.7052	0.0665	-0.0180	-0.0380	0.0983	-0.0701	0.1830	-0.1830	-0.0701	0.0117	0.0380	0.0890
DTL-17/20	0.9480	0.7604	-0.0784	0.0620	-0.2070	0.2160	0.0511	0.0430	0.0430	0.0511	-0.2160	0.2070	0.0620
DTLSC-19/20	0.9720	-0.7483	-0.1065	0.0840	-0.1430	-0.0591	0.0043	0.0100	-0.0098	-0.0043	0.0591	0.0660	0.0680
DTLSC-9/10	0.9 630	-0.6857	-0.0567	-0.0170	0.0340	0.0514	-0.0163	-0.1340	-0.1240	-0.0163	0.0514	0.0160	-0.0060
DTLSC-17/20	0.9480	-0.5852	0.0098	0.0580	0.1880	0.1128	-0.0119	-0.0320	0.0290	0.0119	-0.1128	-0.0870	-0.0210

III. TORQUE RIPPLE HARMONIC ANALYSIS

Parasitic effects such as torque ripple, noise, vibration, and unbalanced magnetic forces are always a concern when designing electrical machines [10]. Pulsating torques also known as torque ripples arise from the interaction of air gap field components which have the same pole number but rotate at different speeds. The magnitude of the torque ripple depends on the product of the magnitude of the two interacting fields, and its frequency on the difference between their speeds [9]. The % torque ripples in table II were obtained using (15).

$$T_{ripple} = \frac{T_{\max} - T_{\min}}{T_{av}} \times 100 \tag{15}$$

Where T_{max}, T_{min} and T_{av} are defined as the maximum, minimum and average torque, respectively. Fig. 5 shows no-load instantaneous torques as function of position and their harmonic spectra. It is clear from the Fourier analysis in fig.5 (b, d, f, h and j) that the dominant torque harmonics are the third and these harmonics torques have the same percentage for the different winding configurations investigated in this paper. They depend on the saturation level on iron parts (stator and rotor teeth, stator and rotor core) of the machine.

As a consequence of iron saturation, the airgap wave changes and new harmonic field are produced which are known as *saturation harmonics* [12]. The main saturation harmonic field is the third. When they interact with other airgap field components which have the same pole number but rotate at different speed they produce torque ripple harmonics.

The torques shown from in fig. 5 (a, c, e, g and i) have been computed from Maxwell's stress tensor. This method requires only the local flux density distribution [11]. The harmonic torque magnitudes in fig.5 (b, d, f, h and j) were computed using Fast Fourier Transform (FFT).

Finite Element Model (FEM) results of all winding configurations have been computed under no-load conditions with the same machine parameters as found in appendix table IV. It is important to note that in the geometries of FEM no space was left out between layers in slots as to avoid introducing additional air-gap harmonic conductance, meaning the slot filling factor is the same for all winding configurations. The Finite Element Software used in this paper is the professional "Quick Field" Version 5.7 from Tera Analysis Ltd.

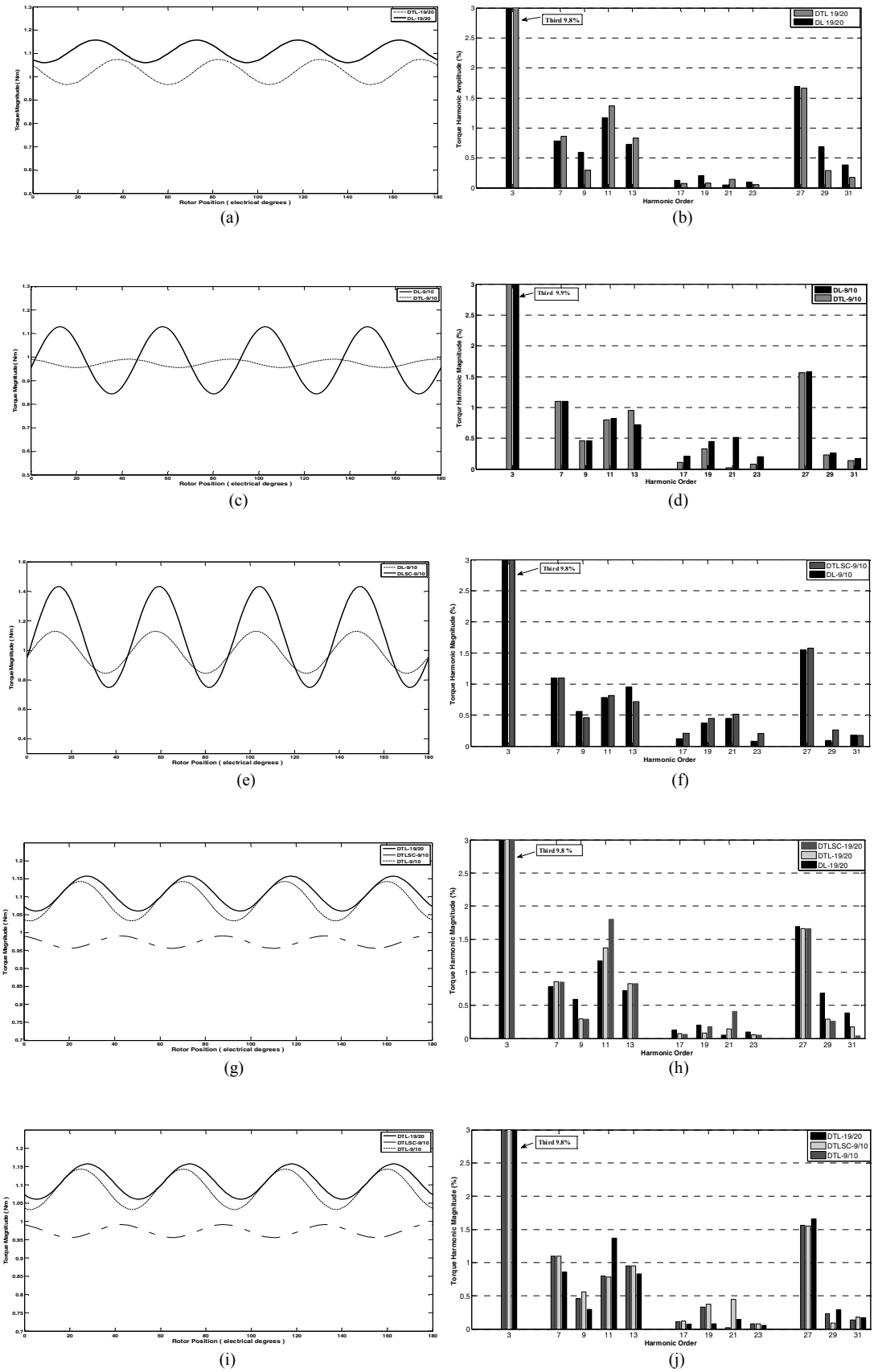

Fig.5. No-load instantaneous torques and their harmonic spectra. (a) Comparison between DTL-19/20 and DL-19/20 no-load instantaneous torques, (b)Fourier series expansion of no-load instantaneous torques for DTL-19/20 Vs DL-19/20 . (c) Comparison between DTL-9/10 and DL-9/10 no-load instantaneous torques, (d)Fourier series expansion of no-load instantaneous torques for DTL-9/10 Vs DL-9/10. (e) Comparison between DTLSC-9/10 and DL-9/10 no-load instantaneous torques, (f)Fourier series expansion of no-load instantaneous torques for DTLSC-19/20 Vs DL-19/20. (g) Comparison between DTL-19/20, DTLSC-19/20 and DL-19/20 no-load instantaneous torques, (h)Fourier series expansion of no-load instantaneous torques for DTL-19/20, DTLSC-19/20 and DL-19/20 . (i) Comparison between the best performing winding configurations no-load instantaneous torques: DTL-19/20 Vs DTL-9/10 Vs DTLSC-9/10, (j)Fourier series expansion of no-load instantaneous torques for DTL-19/20 Vs DTL-9/10 Vs DTLSC-9/10.

Reading from table II, the winding combination with a lower ripple torque is DTL-9/10 but its average no-load torque left to be desired as it drops below 1 Nm. The best winding combination is DTL-19/20 as it has a torque ripple of 8.7 % and a very desirable average no-load torque of 1.109 Nm.

TABLE II
TORQUE RIPPLE AND TORQUE AVERAGE

Winding layouts	q_1-q_2	Torque Ripple	Torque Average
SL-20/20	-	19.1%	1.108 Nm
DL-19/20	-	10.6%	1.021 Nm
DL-9/10	-	28.8%	0.986 Nm
DL-17/20	-	22.0%	0.845 Nm
DLSC-19/20	2	126.9%	0.965 Nm
DLSC-9/10	2	62.8%	1.089 Nm
DLSC-17/20	2	67.9%	0.907 Nm
DTL-19/20	-	8.7%	1.109 Nm
DTL-9/10	-	3.6%	0.974 Nm
DTL-17/20	-	9.1%	0.774 Nm
DTLSC-19/20	1	66.0%	1.040 Nm
DTLSC-9/10	1	10.2%	1.088 Nm
DTLSC-17/20	1	6.3%	0.898 Nm

It is clear from the Fourier analysis that the DTL-19/20 has the lowest first belt-harmonic torque magnitude, which stands at 0.29 % of the fundamental, and the DLSC-17/20 gives the highest first belt-harmonic torque magnitude of 1.7 % of the fundamental.

Table III gives the magnitude of different harmonic torque components. It is noted that the third torque harmonics due to saturation level on iron parts are dominant in all winding configurations and their % values respect to the fundamental torque are almost the same.

The torque as function of rotor position is periodic function. Every periodic and monotonic function can be described by an infinite of harmonic functions of different magnitudes and frequencies. With the torque being the objective function the series can be written as in (16).

$$T = T_{av} + \sum_{n=1}^{\infty} \left[A_n \sin\left(n\theta + \varphi_n\right) \right] \tag{16}$$

TABLE III
HARMONIC TORQUE

Winding Layout	n=1	n=3	n=7	n=9	n=11	n=13	n=17	n=19	n=21	n=23	n=27	n=29	n=31
	Nm	Nm	Nm	Nm	Nm	Nm	Nm	Nm	Nm	Nm	Nm	Nm	Nm
SL-20/20	1.1080	0.1296	0.0159	0.0090	0.0220	0.0072	0.0035	0.0050	0.0020	0.0012	0.0189	0.0050	0.0040
DL-19/20	1.0210	0.1004	0.0080	0.0060	0.0120	0.0074	0.0013	0.0021	0.0005	0.0001	0.0173	0.0070	0.0039
DL-9/10	0.9860	0.0967	0.0112	0.0045	0.0081	0.0071	0.0021	0.0047	0.0035	0.0020	0.0156	0.0026	0.0017
DL-17/20	0.8460	0.0836	0.0132	0.0133	0.0125	0.0023	0.0015	0.0015	0.0013	0.0009	0.0155	0.0003	0.0871
DLSC-19/20	0.9850	0.0969	0.0076	0.0041	0.0209	0.0079	0.0002	0.0031	0.0026	0.0000	0.0155	0.0068	0.0048
DLSC-9/10	1.0890	0.1073	0.0123	0.0063	0.0108	0.0106	0.0006	0.0041	0.0010	0.0008	0.0167	0.0037	0.0023
DLSC-17/20	0.9070	0.0895	0.0132	0.0154	0.0117	0.0067	0.0006	0.0025	0.0019	0.0002	0.0152	0.0008	0.0033
DTL-19/20	1.1090	0.1088	0.0095	0.0033	0.0152	0.0092	0.0008	0.0009	0.0016	0.0006	0.0184	0.0032	0.0019
DTL-9/10	0.9740	0.0965	0.0107	0.0045	0.0078	0.0093	0.0011	0.0032	0.0002	0.0008	0.0152	0.0023	0.0014
DTL-17/20	0.7740	0.0768	0.0110	0.0102	0.0079	0.0055	0.0002	0.0020	0.0010	0.0005	0.0131	0.0007	0.0021
DTLSC-19/20	1.0400	0.1020	0.0089	0.0030	0.0193	0.0087	0.0007	0.0019	0.0043	0.0005	0.0173	0.0027	0.0004
DTLSC-9/10	1.0880	0.1077	0.0119	0.0061	0.0085	0.0104	0.0013	0.0041	0.0049	0.0009	0.0169	0.0010	0.0020
DTLSC-17/20	0.9830	0.0971	0.0131	0.0096	0.0079	0.0102	0.0007	0.0022	0.0012	0.0006	0.0156	0.0020	0.0033

Where

$$A_n = \left(a_n^2 + b_n^2\right)^{1/2} \tag{17}$$

And

$$\varphi_n = \tan^{-1}\left(a_n / b_n\right) \tag{18}$$

And T_{av} is the average torque, a_n and b_n are the magnitudes of the imaginary and real part of the n^{th} harmonic, θ the rotor angle (position), A_n the magnitude and φ_n the angle of the harmonic order n

It is noticeable that the primary sequence first phase-belt torque harmonics "n=9" for best winding combination "DTL-19/20" that mitigates the torque ripple and maintain the average torque high is approximately 0.29 % of its fundamental. Compare to the conventional DL-19/20 where the primary sequence 9th harmonic torque is 0.58% of its fundamental torque. The other performing winding combination is the DTLSC-9/10. The primary sequence first phase-belt harmonic torque for this winding is 0.56 % of its fundamental torque. The less performing winding combination is the DLSC-19/20 with 126.9 % torque ripple.

IV. CONCLUSION

An investigation of the effect of mixing different winding configurations on the torque ripple of a five-phase induction machine has been carried out. It has been pointed out that the combination of double and triple layer can achieve excellent reduction of torque ripple while maintaining the torque average. The machine designer must, however, pay attention to the choosing of the coil pitch. As it is noticed from the results that some double and triple layer winding combinations drop the torque average while reducing the torque ripple. The same can be said for the double and triple layer combined with the slot shift and coil side shift in slots. The approach is valid for any m-phase induction machine of p-poles with integer number of slots per pole and per phase.

This could lead to new winding combinations such as double-four layer winding and simple triple-layer winding depending on the number of stator phases, number of stator slots and number of poles.

The proposed idea in this paper means that the designer needs to make provision for enough space in the slots to accommodate insulation and avoid creating big space between coil sides in a slot.

V APPENDIX

TABLE IV
PARAMETERS OF FIVE-PHASE INDUCTION MACHINE

Parameters	Values
Full load voltage	525.00 V
Full load current	4.38 A
No- load current	1.40 A
Full load output	3.00 kW
No- load output	240.00 W
Steady state frequency	50.00 Hz
Number of poles	2
Number of stator slots	40
Number of rotor bars	33

TABLE V
SPECIAL NOTATIONS OF WINDING CONFIGURATIONS

Winding layouts	Description
SL-20/20	Single-layer winding with unity coil pitch
DL-19/20	Double-layer winding with 19/20 coil pitch
DL-9/10	Double-layer winding with 9/10 coil pitch
DL-17/20	Double-layer winding with 17/20 coil pitch
DLSC-19/20	Double-layer winding with 19/20 coil pitch combined with slot shift and coil side shift in one slot
DLSC-9/10	Double-layer winding with 9/10 coil pitch combined with slot shift and coil side shift in one slot
DLSC-17/20	Double-layer winding with 17/20 coil pitch combined with slot shift and coil side shift in one slot
DTL-19/20	Double- triple - layer winding with 19/20 coil pitch
DTL-9/10	Double- triple - layer winding with 9/10 coil pitch
DTL-17/20	Double- triple - layer winding with 17/20 coil pitch
DTLSC-19/20	Double-triple-layer winding with 19/20 coil pitch combined with slot shift and coil side shift in one slot
DTLSC-9/10	Double-triple-layer winding with 9/10 coil pitch combined with slot shift and coil side shift in one slot
DTLSC-17/20	Double-triple-layer winding with 17/20 coil pitch combined with slot shift and coil side shift in one slot

VI. REFERENCES

[1] Ayman S. Abdel-Khalik and Shehab Ahmed, "Performance evaluation of a five-phase modular winding induction machine", *IEEE Trans, on Industrial Applications*, Vol.59. No.6, pp. 2654-2669, June. 2012.

[2] E. A. Klingshirm, "High phase order induction motors part 1-description and theoretical considerations", *IEEE Trans. Power Apparatus and Systems*, vol. PAS-102, No, Jan 1983.

[3] I. Boldea and S. A. Nasar, "The induction machine handbook", New York, CRC Press, 2002.

[4] A. A. Kadaba, "Design and modeling of a reversible 3-phase to 6-phase induction motor for improved survivability under faulty conditions, *Msc. Dissertation*, Dep. Electrical and Computer. Eng. Milwaukee, Wisconsin, May 2008.

[5] T. M. Jahns, "Improved reliability in solid-state AC drives by means of Multiple Independent phase-drive units". *IEEE Trans, on Industrial Applications*, Vol. IA-16, pp. 321-331, May/June, 1980.

[6] X. B. Bomela and M. J. Kamper." Effect of stator chording and rotor skewing on performance of reluctance synchronous machine", IEEE Trans. Industry Applications, Vol.38 (1), pp 91-100, Jan/Feb 2002.

[7] S.A. Nasar," Handbook of electrical machines". New York: Mc-Craw-Hill, 1987.

[8] D.K Jackson, "Torque ripple compensation for an axial-airgap synchronous motor", Msc. Dissertation. Dep. Electrical. Eng, MIT, Aug. 1994.

[9] A. N. Hanekom, "A torque ripple analysis on reluctance synchronous machine ", *MTech. Dissertation*. Dep. Electrical. Eng, Cape Peninsula University of Technology, Sept. 2006.

[10] A.M. EL-Refaie,"Fractional-slot concentrated-windings synchronous permanent magnet machines: Opportunities and challenges," *IEEE Trans. Ind. Electron.*, Vol.57.No.3, pp. 107-121, May/June, 2010.

[11] J.A. Güemes, A.M. Iraolagoitia, P.Fernández and M.P Donsión, "Comparative study of PMSM with integer-slot and fractional-slot windings. *IEEE, XIXth International Conference on Electrical Machines*.ICEM'2010, Rome, Sept 6-8 , 2010

[12] L. A. Pereira, L. F. A. Pereira, C.C Scharlau, R.S Da Rosa and S Haffner, "Analysis of the influence of saturation on the airgap induction waveform of five-phase induction machines". *XVII Congresso Brasiliero de Automatica.* Sep 12 -16, 2010, Bonito-MS.

VII. BIOGRAPHIES

M. Muteba received the three-year Bachelor's Degree of Applied Science and Technology in electrical engineering (Industrial Applications) from the Higher Technical and Commercial Institute, Lubumbashi, DRC in 1996. After ten years of industrial experience in electrical machines, drives and medium and low voltage power distribution systems, he joined the Tshwane University of Technology and received a B.Tech degree in electrical engineering in 2008.

For the last two years he is teaching courses to undergraduate students at Vaal University of Technology and conducts research in the Energy and Industrial Power Systems at Tshwane University of Technology since 2009. He is at the latest stage of completing his Master's degree of technology. His research interests are electric machines, drive systems and power electronics.

Adisa A. Jimoh (M'86, SM'10) received the B.Eng. and M.Eng. degrees from Ahmadu Bello University (ABU), Zaria, Nigeria, in 1977 and 1980, respectively, and the Ph.D. degree from McMaster University, Hamilton, ON, Canada, in 1986.

He was with ABU until 1992, when he moved to the Research and Development Unit, National Electric Power Authority (NEPA), Lagos, Nigeria. He was with NEPA until 1996 when he moved to the University of Durban-Westville, Durban, South Africa, where he taught courses and carried out research in high-performance energy efficient electric machines and power systems and power electronics. In 2001, he joined Tshwane University of Technology, Pretoria, South Africa, where, as a Full Professor, he is the Head of Department of Electrical Engineering and the leader of the Energy and Industrial Power Systems research niche area. His research interests are in electric machines, drives, and power-electronics applications in power systems.

Dr. Jimoh is a Registered Engineer in South Africa and a NRF rated researcher.

Dan V. Nicolae (M) is with the Tshwane University of Technology Department of Electrical Engineering. He graduated the Polytechnic University of Bucharest, Romania in 1971 with MSC degree and got his doctorate degree in 2004 at Vaal University of Technology, South Africa. After graduation he worked as researcher in the Institute of Nuclear Technologies, National Institute for Scientific and Technological Creativity-Avionics Division, Bucharest, Rumania.

In 1998 he joined the Tshwane University of Technology, Electrical Department, South Africa. He is doing Research in the field of power converters, control of electric machines and applications of power electronics in power systems and renewable energy conversion.